Relative stability of two dimensional hexagonal and square phases of discotic molecules: A theoretical study

Santosh Prasad Gupta* [a], Mukesh Chandra Bos [a], Shallu Dhingra [b] and Santanu Kumar Pal * [b]

[a] Department of Physics, Patna University, Patna-800005,
santosh-phy@patnauniversity.ac.in, drspgpu@gmail.com
[b] Department of Chemical Sciences, Indian Institute of Science Education and Research (IISER) Mohali, Sector-81, SAS Nagar, Knowledge City, Manauli-140306,India.
skpal@iisermohali.ac.in; santanupal.20@gmail.com

ABSTRACT

We have employed a mean field theory, which is a modified Ginzburg-Landau expansion in terms of the scalar order parameter $\Phi(r)$, to stabilize the various ordered phases of the discotic molecules. The $\Phi(r)$ represents the local density differential between the stiff core and the outside alkyl chain regions of the discotic molecules. The current theoretical analysis stabilizes the ordered phases, particularly the square and 2D hexagonal phases. This work also identifies the direct hexagonal and reverse hexagonal phases, with the phases occuring in the following order: $disorder(D)$ - H_I - S_I - H_{II} - $disorder(D)$ with increase in relative concentration, Φ_o. Contrarily, the stability area of the S phase accounts for around 10% of the total area of the ordered phase, whereas the H_I and H_{II} phases each occupy about 45% of the total area of the ordered phase.

KEYWORDS
Discotic, Square Phase, 2d Hexagonal Phase, Order Parameter, Mean field Theory

1. Introduction

One of nature's most efficient methods for creating the dynamic, functional building blocks of life needed to carry out the desired biological activities is molecular self-assembly [1]. Nature uses a variety of supramolecular interactions at various molecular levels to create dynamic functional soft materials, including hydrogen bonding, stacking, polar-nonpolar interactions, metal coordination, charge-transfer complexes, and ionic interactions. Similar to this, supramolecular systems are fascinating from a scientific standpoint since they mimic the complex natural systems. Liquid crystals (LCs) are the standard for self-organizing molecules in use today among a variety of supramolecular systems. Due to their widespread use in laptops, computers, smart phones, digital cameras, MP3 players, flat-panel TVs, and other electronic devices, LCs can be linked to our daily life. Several angles on LCs have been investigated to reduce the cost, space, energy, raw materials, and to boost the stability and efficiency of these LC materials for easy commercialization [2].

LCs are primarily divided into discotic and rod-like (calamitic) mesogens. The discotic LCs, which Chandrasekhar first identified in 1977, differ from their calamitic

counterparts in terms of their molecular structure, phase symmetry, the dimension of their charge transport, exciton migration, and the degree of their orbital overlap [3–7]. The primary building blocks of these discotic systems are rigid aromatic units that are piled on top of one another to create columns that serve as nano-wires. These discotic LCs have extremely high levels of conjugation, which causes the electrons to be substantially delocalized. This results in a smaller band gap, which makes these materials operate as organic semiconductors [8,9].

A typical discotic mesogen has an alkyl side chain that is flexible around a hard, -conjugated aromatic core. These discogens form one-dimensional columns by stacking on top of one another through interactions known as "- stacking." After then, these columns continue to self-organize on different two-dimensional (2D) lattices like hexagonal, rectangular, etc.

The four basic types of mesophase produced by discotic mesogens are the nematic, smectic, columnar, and cubic phases [10–13]. A comparable orientational order to that seen in nematic phases of calamitic LCs is present in the nematic phase of discotic LCs, also known as the discotic nematic (N_D) mesophase. Moreover, discotic mesogens have the ability to stack themselves into short columns that are arranged in their orientation rather than in a two-dimensional positional manner. This indicates that short-range positional order and long-range orientational order are characteristics of discogens in this type of self-assembly. Nematic columnar (N_{Col}) mesophase is the word used to describe these phases

These discotic units can also exhibit smectic phases in a manner that is comparable to how calamitic mesogens exhibit nematic phases in the creation of their mesophases. Although the molecules do not form any columnar aggregates during the discotic smectic phase, the discs are stacked in layers that are divided by sub-layers of peripheral chains [10].

Interestingly, the columnar mesophase is the most frequently observed type of mesophase created by discotic LCs. This is further supported by the fact that discogens mostly comprise -conjugated units, which prefer to organise into columns as a result of –interactions between the discotic units. Different 2D lattices created by one-dimensional columns serve as the basis for differentiating columnar mesophases. The degree of order in the molecular stacking, the orientation of the molecules along the columnar axis, the dynamics of the molecules within the columns, and other variables all play a role in how these varied 2D lattices arise. These columnar LCs can be broadly divided into seven groups, including (i) columnar hexagonal, (ii) columnar rectangular, (iii) columnar oblique, (iv) columnar plastic, (v) columnar helical, and (vi) columnar square (tetragonal) and (vii) columnar lamellar mesophases [10,11,13].

Columns are stacked in a 2D hexagonal lattice in the columnar hexagonal (Col_h) phase. The constituent discs inside the columns can be ordered or disordered, which is reflected in the various values of their correlation lengths. When columns are slanted with respect to the columnar axis, as is the case with columnar rectangular (Col_r) mesophase, the result is an elliptical cross-section of the columns. On a rectangular lattice, these columns are placed. Although the cores of a column should be tilted with regard to the cores of neighboring columns, strong core-core interactions are necessary for the creation of the Col_r phase. Similar to the Col_r phase, the

constituent columns of the columnar oblique (Col_{ob}) mesophase are arranged on a 2D oblique lattice. A three-dimensional arrangement in any of the above mentioned columnar lattices makes up the bulk of the columnar plastic (Col_p) phase. The motional freedom of the discs, which is normally observed in the aforementioned columnar phases, is restricted in the Col_p phase and is only permitted to rotate along the columnar axis. Columnar square or tetragonal (Col_{tet}) represents the mesophase where columns are upright and organized on a square lattice. This mesogen exhibit simple homeotropic alignment of columns. Columns made up of stacked discotic mesogens are grouped in layers in columnar lamellar (Col_L) mesophase. There is no spatial association between the columns of various levels, and layers' columns are free to slide. Cubic phase is the final mesophase variant shown by discotic LCs. In the cubic phase, discotic mesogens are arranged in branched, interlaced columns that form a cubic lattice. In discotic LCs, this phase is seldom ever seen.

The key components of discotic LCs are a central core with a conjugated disc shape that encourages the crystalline character and periphery flexible alkyl chains that make it easier for the liquid character to exist. By altering the size, form, and composition of the central discotic core as well as the type of flexible side chains, it is possible to create discotic LCs with various mesophase morphologies. Or, to put it another way, the discotic molecule can be thought of as a mixture of a rigid core region surrounded by a flexible alkyl chain regime, where the relative concentration of these two regimes controls the mesophase morphologies.

In the current study, the stability of the two-dimensional discotic molecule-based hexagonal and square phases has been examined using modified Ginzburg-Landau theory. For the columnar square and columnar hexagonal phases, respectively, we have used the S and H symbols here and moving forward. The discotic columns are set up in these phases on 2d square and hexagonal lattices, respectively. The order parameter was expanded in a single mode and is expressed in terms of reciprocal lattice vectors corresponding to the first shell. Furthermore, the hexagonal and square phases in the concentration-temperature phase diagram can be stabilized by the current theoretical work. It is discovered that the percentages of the stabilized area for the hexagonal and square phases are, respectively.

This article has the following format. The following part introduces the Ginzburg-Landau free energy functional of a single order parameter, which is used throughout this paper. In section 3, free energy curves for the H and S phases that vary with respect to the relative concentration, Φ_o for various values of the parameters A and B, are calculated once the order parameter has been established. The estimated equilibrium phase diagram was also presented in the A-Φ_o plane. Section 4 marks the conclusion of this section.

2. Theory

To build a Ginzburg-Landau model for the self-assembly of discotic molecules, one must first choose which degrees of freedom in the system are deemed to be crucial and must therefore be included in the model. It goes without saying that there is a scalar order parameter field, $\Phi(r)$, for the local density difference of the two components, the rigid core and the peripheral alkyl chains regions of the discotic molecules.

For the purposes of theoretical computations, these two components can be treated as two regular fluids, and the system of discotic molecules can be viewed as a binary fluid mixing of these two regular fluids with isotropic interactions between all molecules. It receives its averaged free energy density from as:

$$F = \frac{\int f(\Phi(r))dr}{\int dr}$$
$$Where\ f(\Phi(r)) = A\Phi^2(r) + B\Phi^4(r) \tag{1}$$

The free energy density (local) of the homogeneous order parameter, $\Phi(r)$, is expressed as $f(\Phi(r))$. Moreover, A & B are the parameters and they work according to temperature. By integrating $f(\Phi(r))$ over the modulated phase's unit cell and then dividing the result by the cell's size, one can obtain the averaged free energy density (F). As a result, the unit of F and the unit of free energy density $f(\Phi(r))$ are the same. This free energy has also been utilized to explain a variety of systems, including magnetic layers [14], Langmuir films [15], diblock copolymers [16], and micro-emulsions [17]. Also, this free energy function is quite general and has no bearing on any particular system.

3. Results and Discussion

3.1. Order parameter for different phases

In our model, ordered phases can become stable if the strength of the core-core and alkyl chains-core interactions is strong enough. We continue searching for configurations that minimize the free energy density functional, F [Eq. 1]. The order parameter field, $\Phi(r)$, is extended in a Fourier series as

$$\Phi(r) = \Phi_o + \sum_{i=1}^{i=N} \sum_{k\ \epsilon\ S_i} \Phi_k(r)\ Cos(\vec{G}.\vec{r}) \tag{2}$$

$\Phi(r)$ is made up of the modulated term and the constant term, Φ_o. Φ_o is the concentration of the discotic molecule's rigid core region relative to the alkyl chain and is defined as follows:

$$\Phi_o = C_{alkyl\ chain} - C_{core}$$

, where $C_{alkyl\ chain}$ is the average concentration of the alkyl chain part and C_{core} is the average concentration of the rigid core of the discotic molecule. Also, it is necessary to note that the electron density of the core region is higher than that of the alkyl chain portion. further, it must be remembered that this cannot be directly compared to the real system. In the modulated term, $\vec{G}$ stands for the reciprocal vectors, and $\Phi_k(r)$ is the corresponding Fourier or scattering amplitude . S_i signifies the $i-th$ cell of the reciprocal vectors. Only those reciprocal vectors that correspond to the first cell of the reciprocal lattice have we employed in this case. Now, our focus is on determining how stable the columnar square (S) and columnar hexagonal (H) phases are in comparison. These phases are projected on two dimensions to produce

square and hexagonal lattices, respectively. Nonetheless, the disorder phase (D) is also included in our study for reference.

For the disorder, square, and two dimensional hexagonal phases, let's designate the scalar order parameter as $\Phi_D(r)$, $\Phi_S(r)$, & $\Phi_H(r)$, respectively. In the disorder phase, the modulated portion of the order parameter is zero because, as implied by the phase's name, the value of the order parameter is roughly constant throughout the unit cell. Because there is just one Φ_o term in the $\Phi_D(r)$, the expression for the $\Phi_D(r)$ can be written as follows:

$$\Phi_D(r) = \Phi_o \tag{3}$$

In the case of the S phase, let's assume that the lattice parameter is a_s. Thereafter, direct basis vectors can be expressed as;

$$\vec{a} = a_s\hat{i} \quad \& \quad \vec{b} = a_s\hat{j}$$

resulting in the reciprocal basis vectors being;

$$\vec{a^*} = \frac{2\pi}{a_s}\hat{i} \quad \& \quad \vec{b^*} = \frac{2\pi}{a_s}\hat{j}$$

As is well known, the reciprocal lattice vector is represented by;

$$\vec{G} = h\vec{a^*} + k\vec{b^*}$$

Hence, after accounting for the values of a^* and b^* in the relationship above, we have

$$\vec{G} = \frac{2\pi}{a_s}[h\hat{i} + k\hat{j}]$$

Where h and k are the Miller indices of the reflecting planes of square lattice. As a result, the reciprocal lattice vectors in the first cell of the reciprocal lattice corresponding to square lattice are as follows [Fig. 1[i] & [ii]]:

$$\vec{G}_{10} = \frac{2\pi}{a_s}\hat{i}, \quad \vec{G}_{\bar{1}0} = -\frac{2\pi}{a_s}\hat{i}, \quad \vec{G}_{01} = \frac{2\pi}{a_s}\hat{j}, \quad \vec{G}_{0\bar{1}} = -\frac{2\pi}{a_s}\hat{j}$$

and as a result the expression of the $\Phi_S(r)$ can be stated as follows:

$$\Phi_S(r) = \Phi_o + A_S\ [Cos(\frac{2\pi x}{a_s}) + Cos(\frac{2\pi x}{a_s})] \tag{4}$$

Where, A_S is the scattering (Fourier) amplitude corresponding to the square lattice.

Similar to this, let's assume that the lattice parameter in the hexagonal phase is a_h. Direct basis vectors are then represented as;

$$\vec{a} = a_s\hat{i} \quad \& \quad \vec{b} = a_s\hat{j}$$

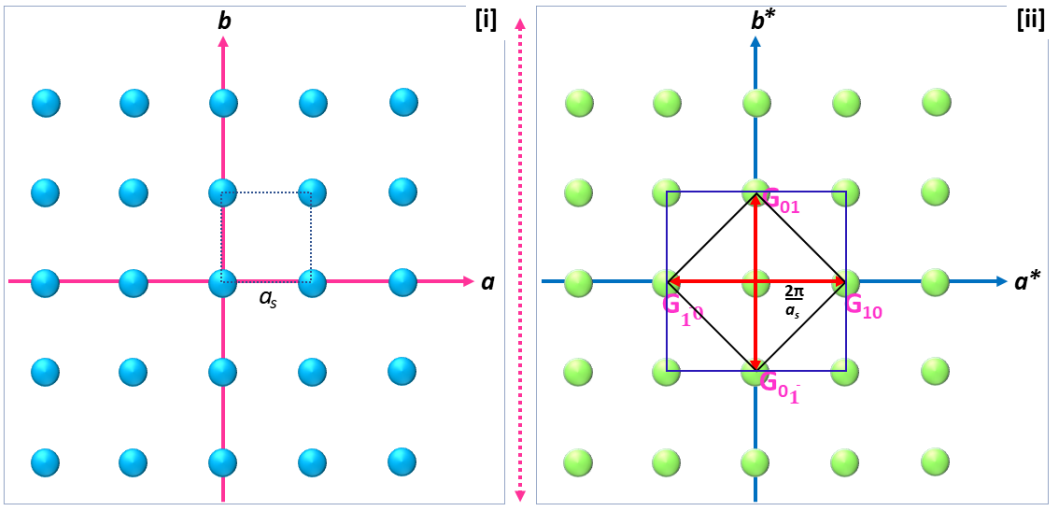

Figure 1. [i] showing the direct square lattice where a_s is the lattice parameter [ii] Reciprocal lattice corresponding to the square lattice. Rhombus in black color denote the first cell and square in blue color represents the second cell in the reciprocal space. The red colored vectors ($\vec{G}_{10}, \vec{G}_{\bar{1}0}, \vec{G}_{01}$&$\vec{G}_{0\bar{1}}$) correspond to the reciprocal vectors in the first cell.The square in blue color correspond to the second cell.

as a result, the reciprocal basis vectors are;

$$\vec{a^*} = \frac{2\pi}{a_h}(\hat{i} + \frac{\hat{j}}{\sqrt{3}}) \quad \& \quad \vec{b^*} = \frac{4\pi}{a_h\sqrt{3}}\hat{j}$$

Hence, after taking into account the values of a^* and b^*, we have

$$\vec{G} = \frac{2\pi}{a_h}[h\hat{i} + (\frac{h}{\sqrt{3}} + \frac{2k}{\sqrt{3}})\hat{j}]$$

As a result, the reciprocal lattice vectors in the first cell of the reciprocal lattice that corresponds to the two-dimensional hexagonal lattice are as follows [Fig. 2[i] & [ii]]:

$$\vec{G}_{10} = \frac{2\pi}{a_h}(\hat{i} + \frac{\hat{j}}{\sqrt{3}}), \quad \vec{G}_{\bar{1}0} = -\frac{2\pi}{a_h}(\hat{i} + \frac{\hat{j}}{\sqrt{3}}), \quad \vec{G}_{01} = \frac{4\pi}{a_h\sqrt{3}}\hat{j}, \quad \vec{G}_{0\bar{1}} = -\frac{4\pi}{a_h\sqrt{3}}\hat{j}$$

$$\vec{G}_{1\bar{1}} = \frac{2\pi}{a_h}(\hat{i} - \frac{\hat{j}}{\sqrt{3}}), \quad \vec{G}_{\bar{1}1} = -\frac{2\pi}{a_h}(\hat{i} - \frac{\hat{j}}{\sqrt{3}}),$$

and as a result, the $\Phi_H(r)$ expression can be written as follows:

$$\Phi_H(r) = \Phi_o + A_H\ [Cos\frac{2\pi}{a_h}(x + \frac{y}{\sqrt{3}}) + Cos\frac{4\pi}{a_h}(\frac{y}{\sqrt{3}}) + Cos\frac{2\pi}{a_h}(x - \frac{y}{\sqrt{3}})] \qquad (5)$$

Where, A_H is the scattering (Fourier) amplitude corresponding to the two dimensional hexagonal lattice.

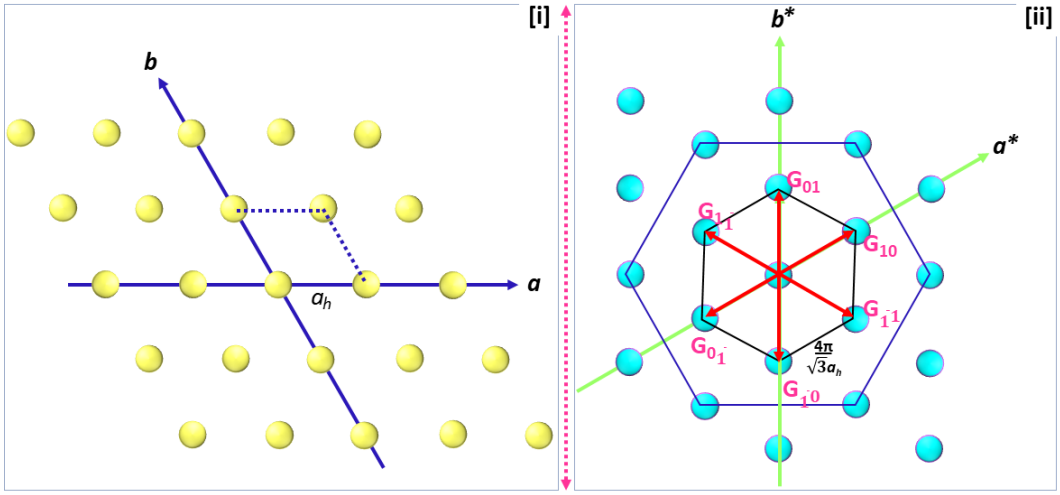

Figure 2. [i] Display direct two dimensional hexagonal lattice where a_h is the lattice parameter [ii] shows a lattice that is reciprocal to the hexagonal lattice. In the reciprocal space, the first cell is represented by a hexagon in black, while the second cell is shown by a hexagon in blue that has been rotated by 30 degrees with respect to the first one. The vectors; $\vec{G}_{10}, \vec{G}_{\bar{1}0}, \vec{G}_{01}, \vec{G}_{0\bar{1}}, \vec{G}_{1\bar{1}}$ & $\vec{G}_{\bar{1}1}$ in red color correspond to the reciprocal vectors in the first cell.

3.2. Free energy for different phases

Combining the three equations [3, 4, 5] we obtain

$$\Phi_D(r) = \Phi_o \tag{6a}$$

$$\Phi_S(r) = \Phi_o + A_S\ [Cos(\frac{2\pi x}{a_s}) + Cos(\frac{2\pi y}{a_s})] \tag{6b}$$

$$\Phi_H(r) = \Phi_o + A_H\ [Cos\frac{2\pi}{a_h}(x + \frac{y}{\sqrt{3}}) + Cos\frac{4\pi}{a_h}(\frac{y}{\sqrt{3}}) + Cos\frac{2\pi}{a_h}(x - \frac{y}{\sqrt{3}})] \tag{6c}$$

By substituting the $\Phi(r)'s$ of the phases from equation [6] into equation [1], the expression of free energy density (F) of the aforementioned phases is derived. Let's use the symbols F_D, F_S, and F_H to designate free energy density of the disorder, square, and two-dimensional hexagonal phases, respectively. Then we have

$$F_D(A, B, \Phi_o) = A\ \Phi_o^2 + B\ \Phi_o^4 \tag{7a}$$

$$F_H(A, B, \Phi_o) = A\ \Phi_o^2\ + B\ \Phi_o^4\ +\ \frac{3}{8}\ A_H^2\ (4A\ +\ B(15\ A_H^2\ +\ 16\ A_H\ \Phi_o\ +\ 24\ \Phi_o^2)) \tag{7b}$$

$$F_S(A, B, \Phi_o) = A\ \Phi_o^2 + B\ \Phi_o^4 + \ A\ A_S^2 + \frac{1}{4}(9B\ A_S^4)\ +\ 6B\ A_S^2\ \Phi_o^2 \qquad (7c)$$

Each phase's free energy density has four variational parameters, A, B, Phi o, and the Fourier amplitude. Free energy density is minimised with regard to the Fourier amplitude of each phase for each combination of A, B, and Φ_o. And for that set of variational characteristics, the phase with the lowest energy is stable.

3.3. Free energy curves

Figures [Fig. 3] depict the variations in the free energy density of the various phases with regard to Φ_o at various values of A & B. In this case, the free energy was estimated for $B = 1$ and $B = 5$, and the value of A was set at $0, -0.5, -1, -3, -5$, and 7 for each value of B.

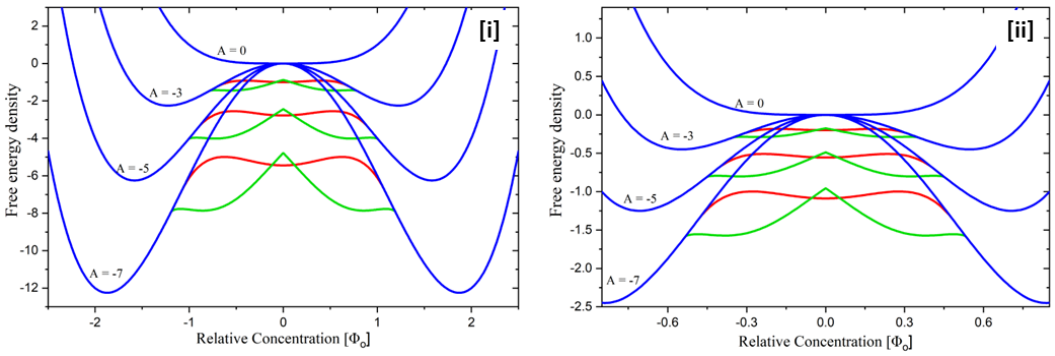

Figure 3. Variation of free energy density for the square (S), Hexagonal (H) and disorder (D) phases with respect to average concentration (Φ_o) at the value of parameter [i] $B = 1$ and [ii] $B = 5$. For each value of B the value of parameter $A = 0, -3, -5, -7$, curve in red, green, & blue colors correspond to square (S), Hexagonal (H) and disorder (D) phases, respectively.

According to the figures [Fig. 3], the free energy variation with respect to Φ_o in the case of the square phase contains one minima at $\Phi_o = 0$ and two additional minima symmetrically positioned about $\Phi_o = 0$, one at the positive side and one at the negative side of Φ_o. As seen in the figure, the value of the free energy corresponding to these minima rises as A increases, while the distance between the two symmetrical minima reduces and eventually combines to form the minima at $\Phi_o = 0$. The free energy curve for the hexagonal phase, on the other hand, contains two deep minima that are symmetrically located near $\Phi_o = 0$ and on each side of $\Phi_o = 0$. The value of the free energy corresponding to these minima and cusp grows as A is increased in value. However, as seen in the images [Fig. 3], the minimum and cusp were ultimately discovered to be merging and changing into a minima at $\Phi_o = 0$. Moreover, the disorder phase's free energy curve features two symmetric minima located around $\Phi_o = 0$ and one maxima at $\Phi_o = 0$. As the value of A rises, so does the value of the free energy corresponding to these peaks and minima. Yet, at $\Phi_o = 0$, these minima and maxima combine to form a single minima, as seen in the figures [Fig. 3]. Moreover, for $B = 5$, the shape of the free energy density curves for the square (S), hexagonal (H), and disorder (D) phases is identical to that at B = 1. Yet, it is discovered that the stability range of the ordered phases (H, & S) in the Φ_o is smaller at $B = 5$ than it is at $B = 1$.

3.4. Phase diagram : Φ_o -A plane

The diagrams [Fig. 3] make it evident that the square (S) phase has the lowest free energy density of all the phases at and very close to $\Phi_o = 0$. Additionally, the hexagonal phase (H) is stable when one moves away from $\Phi_o = 0$ on either side. Nevertheless, all of these free energy curves eventually combine to form the disorder phase either by departing from $\Phi_o = 0$ very far or by raising the value of A for each increase in B. As a result of the findings made above, it can be said that on either side of the point where $\Phi_o = 0$, the initial square phase stabilizes, followed by the hexagonal phase, and then the disorder phase eventually takes control. The stability area of the ordered phases, S, H, in the Φ_o - A plane of the phase diagram also declines with rising A value and eventually becomes zero at $A = 0$. As a result, the disorder phase entirely took control of the orderly phase at $A = 0$. Yet, behavior at $B = 5$ is quite similar to that at $B = 1$, although the ordered phase's stability zone in the Φ_o - A plane is shorter. From the free energy curves for different values of A and for $B = 1$ and $B = 5$, the (Φ_o, A) coordinates of the square-hexagonal and hexagonal-disorder phase boundaries have been computed, and they are listed in the [Tab. 1] and [Tab. **??**], respectively. Plotting these coordinates as A against Φ_o yields the phase diagram [Fig. 4].

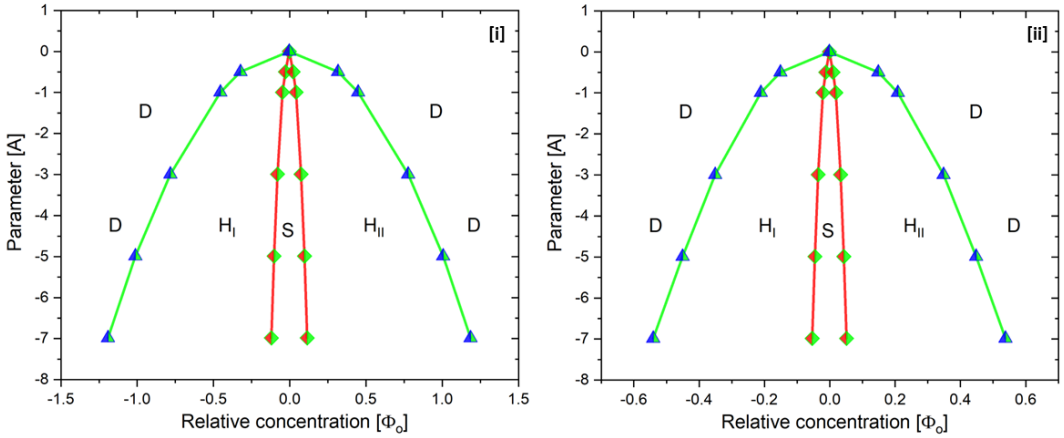

Figure 4. Phase diagram in the $A - \Phi_o$ plane at $B = 1$. S, H_I, H_{II} and D correspond to square, hexagonal(direct), hexagonal(inverse), and disorder phases, respectively.

In order to comprehend the nature of these ordered phases, H & S, related scattering amplitudes, A_H & A_S, have been calculated at $A = -7$, $B = 1$ & $A = -7$, $B = 5$ and at various values of Φ_o included in these phase region [Fig. 5[i]]. The calculated value of scattering amplitude (A_H) for the H phase is discovered to be positive for the negative value of Φ_o. Including the value of A_H into $\Phi_H(r)$ and creating the matching contour plot afterwards results in a pattern where the only region that may display the 2d hexagonal lattice is one with the highest electron density [Fig. 5[i] & 6[i]]. This is the columns of core distributed in the matrix of the alkyl chain on the hexagonal lattice; as a result, the phase is direct hexagonal and is represented by the symbol H_I. For instance, [Fig. 6[i]] displays the contour plot of $\Phi_H(r)$ at $A = -7$, $B = 1$, and $\Phi_o = -0.5$ with an optimal value of $A_H = 1.07939$. In the H phase region, it is also discovered that the value of A_H is negative for the positive value of Φ_o. After adding the A_H value, the accompanying contour plot of $\Phi_H(r)$ displays a pattern where only

Table 1. (Φ_o, A) coordinates corresponding to the phase boundaries; Square-Hexagonal, & Hexagonal-Disorder with accuracy in Φ_o is ± 0.0002 at $B = 1$ and $B = 5$.

$B = 1$				$B = 5$			
Square-Hexagonal		Hexagonal-Disorder		Square-Hexagonal		Hexagonal-Disorder	
Φ_o	A	Φ_o	A	Φ_o	A	Φ_o	A
-0.1178	-7	-1.1901	-7	-0.0527	-7	-0.5400	-7
-0.0996	-5	-1.0100	-5	-0.0444	-5	-0.4500	-5
-0.0771	-3	-0.7801	-3	-0.0344	-3	-0.3501	-3
-0.0444	-1	-0.4520	-1	-0.0199	-1	-0.2100	-1
-0.0252	-0.5	-0.3200	-0.5	-0.0113	-0.5	-0.1500	-0.5
0	0	0	0	0	0	0	0
0.0252	-0.5	0.3200	-0.5	0.0113	-0.5	0.1500	-0.5
0.0444	-1	0.4520	-1	0.0199	-1	0.2100	-1
0.0771	-3	0.7801	-3	0.0344	-3	0.3501	-3
0.0996	-5	1.0100	-5	0.0444	-5	0.4500	-5
0.1178	-7	1.1901	-7	0.0527	-7	0.5400	-7

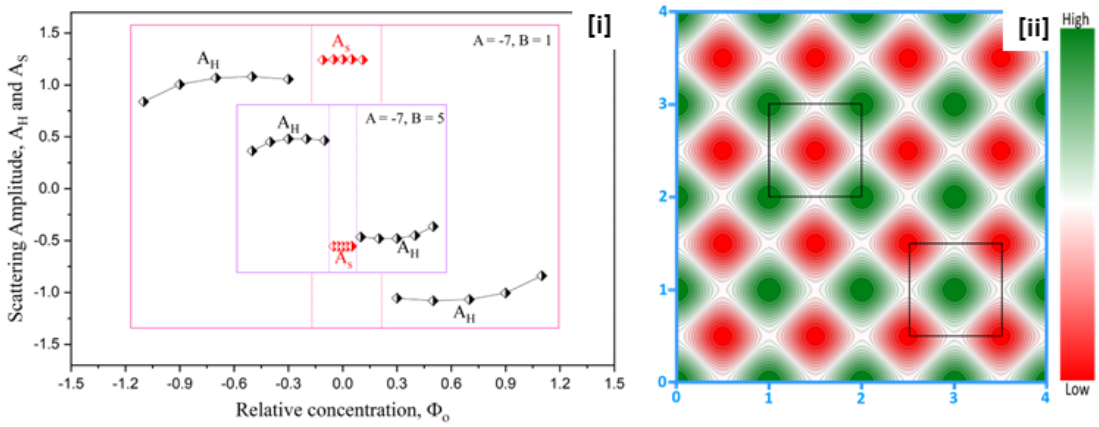

Figure 5. [i] Showing the variation in the scattering (Fourier) amplitudes A_H and A_S in relation to Φ_o in their respective phases. The purple box in inset is associated with parameter $A = -7$ & $B = 5$, while the red box in the inset is related to parameter $A = -7$ & $B = 1$. The scattering amplitude, A_H, is represented by the half-filled diamond in black, and the scattering amplitude, A_S, by the half-filled diamond in red. [ii] Contour plot of $\Phi_S(r)$ at $A = -7$, $B = 1$, and $\Phi_o = -0.05$ with optimal value of $A_S = 1.24588$; deep red hue corresponds to highest electron density, and deep green is the lowest. Scale is given in the unit of the lattice parameter. The square lattice's unit cell is represented by a square. The square lattice can be found in regions with low electron densities as well as with the high electron densities.

the regions with the lowest electron density may exhibit the 2d hexagonal lattice. The phase is reverse hexagonal and is indicated by the symbol H_{II} since this is the columns of alkyl chains distributed on the hexagonal lattice in the core matrix. [Fig. 6[ii]] provides an illustration of the contour plot of $\Phi_H(r)$ at $A = -7$, $B = 1$, and $\Phi_o = 0.5$ with an optimal value of $A_H = -1.07939$.

As opposed to this, it is discovered that the estimated scattering (Fourier) amplitude, A_S, in the square phase, S, for the negative value of Φ_o is the same as that of the corresponding positive value of Φ_o [Fig.5[ii]]. As a result, the contour plot of $\Phi_S(r)$ after accounting for the value of A_S shows the same pattern for positive Phi_o and the

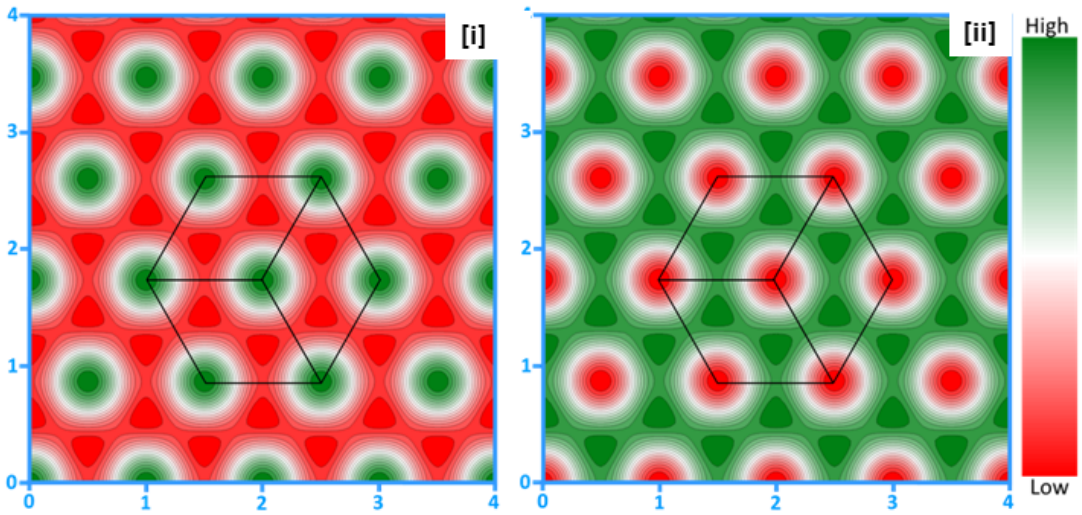

Figure 6. [i] Displaying the contour plot of $\Phi_H(r)$ at $A = -7$, $B = 1$, $\Phi_o = -0.5$ with optimal value of $A_H = 1.07939$, where the only region that may display the 2d hexagonal lattice is that with the highest electron density. [ii] In the contour plot of $\Phi_H(r)$ at $A = -7$, $B = 1$, and $\Phi_o = 0.5$ with optimal value $A_H = -1.07939$, only region with the lowest electron density may exhibit the 2d hexagonal lattice. Scale is given in the unit of the lattice parameter. The hexagon in the black color is the conventional unit cell of the 2d hexagonal lattice. The conventional unit cell is consists of three primitive unit cells.

equivalent negative Phi_o. For instance, [Fig.5[ii]] displays a contour plot of $Phi_H(r)$ at $A = -7$, $B = 1$, and $\Phi_o = -0.05$ with an optimum value of $A_S = 1.24588$. It should be noticed that the contour plot of $\Phi_H(r)$ with optimal values of $A_S = 1.24588$ and $A = -7$, $B = 1$, and $\Phi_o = 0.05$ is identical to the one before. Also, the contour map shows an indivisible square lattice formed by the regions with the lowest and highest electron densities. This is the core columns scattered on the square lattice in the alky chain matrix, or one might say that the alkyl chain columns are spread out on the square lattice in the core matrix.

In conclusion, we may state that the disorder (D) phase, is the initial phase that occurs when value of Φ_o is low. The H_I phase, where columns of core are placed on the 2d-hexagonal lattice in the matrix of alkyl chains, is however brought about by an increase in the value of Φ_o. As Φ_o continues to rise in value, the S phase results. If the value of Φ_o is increased further, the phase changes into the H_{II} phase, which includes columns of alkyl chains arranged on a 2D hexagonal lattice in the matrix of the core. The disorder (D) phase results from further increases in the value of Φ_o. Therefore, the current theoretical study stabilizes the different ordered phases in the following order: $disorder(D)$ - H_I - S_I - H_{II} - $disorder(D)$ as the relative concentration, Φ_o, increases.

Additionally, by fitting the phase boundaries, the stability region of the ordered phases H_I, S, and H_{II} in the $A - \Phi_o$ plane may be estimated. The quadratic equation shown below is determined to best reflect the phase boundaries:

$$A = C\ \Phi_o^2 \tag{8}$$

Where C is the parameter and the corresponding symbols for the phase boundaries of hexagonal- and square-disorders are CH and CS, respectively. These parameters' best-fit values were $C_H = -4.93$ & $C_S = -504.72$ for $B = 1$ and $C_H = -24.23$ & $C_S = -2527.67$ for $B = 5$, respectively. Let's use $Area_{HI}$, $Area_S$, & $Area_{HII}$ to represent the stability areas of the H_I, S, and H_{II} phases in the A - Φ_o plane, respectively. The following integration expression can be used to determine the necessary area:

$$Area_S = \int_{-A}^{0} \Phi_o \, dA = \int_{-A}^{0} \sqrt{\frac{A}{C_S}} \, dA \tag{9a}$$

$$Area_{HI} = \frac{1}{2}[\int_{-A}^{0} \sqrt{\frac{A}{C_H}} \, dA - \int_{-A}^{0} \sqrt{\frac{A}{C_S}} \, dA] \tag{9b}$$

$$Area_{HII} = \frac{1}{2}[\int_{-A}^{0} \sqrt{\frac{A}{C_H}} \, dA - \int_{-A}^{0} \sqrt{\frac{A}{C_S}} \, dA] \tag{9c}$$

Due to the fact that all these ordered phases turn off at $A = 0$ and turn on for negative values of A, the upper and lower integration limits were determined to be 0 and $-A$, respectively. Using the values of C in equation [Eq. 9], the stabilized areas are determined. The computed areas for $B = 1$ are determined to be as follows: $Area_{HI} = 0.1353 \; A^{\frac{3}{2}}$, $Area_S = 0.0297 \; A^{\frac{3}{2}}$, & $Area_{HII} = 0.1353 \; A^{\frac{3}{2}}$ The stability area ratio is approximately: $Area_{HI} : Area_S : Area_{HII} = 1 : 0.22 : 1$. Similar areas calculated for $B = 5$ are found to be $Area_{HI} = 0.0611 \; A^{\frac{3}{2}}$, $Area_S = 0.0133 \; A^{\frac{3}{2}}$, & $Area_{HII} = 0.0611 \; A^{\frac{3}{2}}$. The stability area ratio is around $Area_{HI} : Area_S : Area_{HII} = 1 : 0.22 : 1$. This demonstrates that the S phase occupies roughly 10% of the overall area of the ordered phase, whereas the H_I and H_{II} phases each occupy around 45% of the total ordered phase area.

4. Conclusions

The ordered phases, notably the square and 2D hexagonal phases, are stabilized by the current theoretical analysis. Moreover, the direct hexagonal and reverse hexagonal phases are identified in this work, with the phases occurring in the following order: $disorder(D)$ - H_I - S_I - S_{II} - H_{II} - $disorder(D)$ with rise in relative concentration, Φ_o. Contrarily, the H_I and H_{II} phases each take up about 45% of the overall area of the ordered phase, while the stability area of the S phase is roughly 10% of the entire area of the ordered phase.

5. Acknowledgments

S. P. Gupta thanks Patna University for its technical assistance. S. P. Gupta thanks SERB-TARE (TAR/2021/000146) for the fellowship and the funding.

References

[1] Israelachvili, Intermolecular and surface forces, Academic Press, London 2nd ed. (1991).

[2] B. R. Kaafarani, Discotic liquid crystals for opto-electronic applications, Chem. Mater. 23, 3 (2011) 378–396. doi:doi.org/10.1021/cm102117c.

[3] S. Chandrasekhar, G. S. Ranganath, Discotic liquid crystals, Rep. Prog. Phys. 53 (1990) 57. doi:10.1088/0034-4885/53/1/002.

[4] T. Geelhaar, K. Griesar, B. Reckmann, 125 years of liquid crystals-a scientific revolution in the home, Angew Chem Int Ed. 52 (2013) 8798–8809. doi:10.1002/anie.201301457.

[5] K. Arakawa, Liquid crystal display having positive and negative birefringent compensator films, US005189538A (1993).

[6] H. Mori, Y. Ito, Liquid crystal display with compensators having minimum retardations in the inclined direction, US005189538A (1998).

[7] N. Boden, J. Clements, B. Movaghar, Fluid sensing device using discotic liquid crystals, US006423272B1 (2002).

[8] W. P. S. Sergeyev, Y. H. Geerts, Discotic liquid crystals: a new generation of organic semiconductors, Chem. Soc. Rev. 36 (2007) 1902–1929. doi:10.1039/B417320C.

[9] W. Pisula, K. Mullen, J. W. Goodby, P. J. Collings, T. Kato, C. Tschierske, H. F. Gleeson, P. Raynes, Eds.: Wiley-vch; weinheim 8 (2002) 627–674.

[10] S. Kumar, Self-organization of disc-like molecules: chemical aspects, Chem. Soc. Rev 35 (2006) 83–109. doi:10.1039/B506619K.

[11] T. Shimogaki, S. Dei, K. Ohtab, A. Matsumoto, Columnar mesophases constructed by hierarchical self-organization of rod-like diacetylene molecules, J. Mater. Chem. 21 (2011) 10730–10737. doi:10.1039/C1JM10817D.

[12] C. Tschierske, Micro-segregation, molecular shape and molecular topology –partners for the design of liquid crystalline materials with complex mesophase morphologies, Journal of Materials Chemistry 11(11) (2001) 2647–2671. doi:10.1039/B102914M.

[13] I. Bala, J. De, S. K. Pal, Chapter: Functional discotic liquid crystals through molecular self-assembly: Toward efficient charge transport systems, (part of the book: Nanostructure Science and Technology) (2021). doi:10.1007/978-981-16-4189-3_5.

[14] T. Garel, S. Doniach, Phase transitions with spontaneous modulation-the dipolar ising ferromagnet, Phys. Rev. B 26 (1982) 325–329. doi:10.1103/PhysRevB.26.325.

[15] D. Andelman, F. Broçhard, J. F. Joanny, Phase transitions in langmuir monolayers of polar molecules, J. Chem. Phys. 86 (1987) 3673–3681. doi:10.1063/1.451970.

[16] I. W. Hamley, The physics of block copolymers, Oxford University Press: New York (1999).

[17] G. Gompper, M. Schick, Correlation between structural and interfacial properties of amphiphilic systems, Phys. Rev. Lett. 65 (1990) 1116–1119. doi:10.1103/PhysRevLett.65.1116.